Two-Channels Thermal Energy Storage Tank: Experiments and Short-Cut Modelling

M. Capocelli, A. Caputo, M. De Falco, D. Mazzei, V. Piemonte

***Abstract*—**This paper presents the experimental results and the related modeling of a thermal energy storage (TES) facility, ideated and realized by ENEA and realizing the thermocline with an innovative geometry. Firstly, the thermal energy exchange model of an equivalent shell & tube heat exchanger is described and tested to reproduce the performance of the spiral exchanger installed in the TES. Through the regression of the experimental data, a first-order thermocline model was also validated to provide an analytical function of the thermocline, useful for the performance evaluation and the comparison with other systems and implementation in simulations of integrated systems (e.g. power plants). The experimental data obtained from the plant start-up and the short-cut modeling of the system can be useful for the process analysis, for the scale-up of the thermal storage system and to investigate the feasibility of its implementation in actual case-studies.

***Keywords*—**Thermocline, modelling, heat exchange, spiral, shell, tube.

I. INTRODUCTION

RENEWABLE energy sources are often associated with intermittent productions or in any case temporarily unrelated to energy demand and breakthrough innovations are needed in the energy storage sector to increase the share of non-fossil energy in the grid. The use of thermal energy storage is very important for the practical use of solar energy. Indeed, if equipped with a thermal storage system, the Concentrating Solar Power (CSP) plants represent a mature technology which responds to many of the paradigms of thermoelectric production in terms of flexibility with no emission [1], [2]. The levelized cost of energy (LCOE) ranges between 200USD/MWh (high DNI, 6 hours storage) and 330USD/MWh (low DNI no storage) in the most representative case of Parabolic Trough (PT) [3], [4]. Several plants (capacity of 50-250 MW) have been realized, mainly in Spain and USA, since 2007and now also Abu Dhabi, an oil-rich nation, funded the installation of a 100 MW CSP plant (by Masdar) with Abengoa's PT collectors for a world installed capacity of more than 4.8 GW [5], [6]. In order to further increase the energy world capacity, the LCOE must be lowered and many improvements are needed mainly in the flexibility and availability of these plants. Thermal Energy Systems (TES) can be designed to store energy when abundant and to release it for energy production [5]-[7] space heating/ cooling [8], [9] as well as for freshwater production in desalination systems powered by waste heat or solar energy [2], [10], [11].

As aforementioned, in the framework of energy production, the solar thermal energy still needs some technological improvements to reduce the gap with the fossil fuel sources in terms of LCOE. Although CSP has reached technological maturity, high capital investment and specific electricity cost remain the major development barriers (7000-10000 USD/kW of investment cost depending on the storage capacity [4]). To reduce them, highly efficient, integrated, and cheaper components are needed [7], [12]. Recently, strong efforts are been made to develop alternative storage systems with respect to conventional molten salt (MS) two-tank system in order to gain high cost reduction potential [1], [12]-[14]. One of these concepts is the thermocline single-tank storage that realizes the separation of the salt volumes by density differences between the hot and cold salt volumes. Clearly, this concept presents intrinsic challenges in terms of control, power plant integration and efficiency [12].

Several experimental and modelling works appeared in the recent literature, including both complex rigorous numerical modelling and short-cut mathematical analysis, useful to give practical information with low time-consuming simulations.

Hernandez-Arriaga et al. developed and tested a one-dimensional model of a MS thermocline storage tank with fully inclusion of the boundary conditions [15]. Shin et al. developed a computer program to study the thermal stratification of a storage tank and to provide the process optimization and basic design [16]. By studying a TES discharging process to an integrated steam generator, Rivas et al. simulated the stratification temperature profile through a 2-D axisymmetric transient model with constant boundary conditions [17].

Bayon and Rojas presented the analytical function describing the behaviour of a thermocline storage tank to perform long-term simulations of the power plant [9] and proposed a short-cut one-dimensional approach by means of the Logistic Cumulative Distribution Function (CDF) in order to describe the thermocline behavior during dynamic processes of charge/discharge (without implementing rigorous numerical modelling) [18]. Within this conceptual framework, Pizzolato et al. proposed a reduced model based on the logistic curve, which parameters have been obtained using the results of multiple turbulent simulations obtained from a CFD model [19].

M. Capocelli, M. De Falco and V. Piemonte are with the University Campus Biomedico of Rome, Via Alvaro del Portillo, 21, 00128 Rome, Italy (e-mail: m.capocelli@unicampus.it; m.defalco@unicampus.it; v.piemonte@unicampus.it).

A. Caputo and D. Mazzei are with ENEA (Italian National Agency for New Technologies, Energy and Sustainable Development), Casaccia Research Centre, via Anguillarese 310, 00123 Rome, Italy (e-mail: alberto.caputo@enea.it; domenico.mazzei@enea.it).

World Academy of Science, Engineering and Technology
International Journal of Energy and Environmental Engineering
Vol:11, No:10, 2017

The "CSP Research Group" at ENEA is working on efficient low-cost thermal storage to increase the dispatchability and the flexibility of solar power plants and to reduce the specific cost of electricity [17]. They recently have developed a Thermocline Storage Tank including two spiral heat exchangers submerged in the heat transfer fluid and two isolated channels to facilitate the natural circulation of the tank and to speed-up the formation of the Thermocline. The system has been though to serve the power storage and control between the energy source and the user. The hot source can be seen as the hot diathermic oil coming from the solar field (e.g. Fresnel collectors) and the cold source is the fluid of the power cycle (e.g. organic rankine cycle in case of electricity production).

In this work, we present the experimental results related to the prototype start-up in terms of temperature distribution during the time. Therefore, we validate a simplified thermal exchange model capable of implementing the classic approach of Kern [20] to the spiral exchangers installed inside the TES. This approach allows generating a simple and intuitive correlation between the heat transfer coefficient and the charge/discharge power. Moreover, a reduced order model of the thermocline is validated and utilized to discuss the thermal performance of the TES.

II. PROTOTYPE DESCRIPTION AND EXPERIMENTS

The sketch of the prototype is available in Fig. 1. It includes a cylindrical tank with two submerged spiral exchangers, each connected to a circulation channel. The establishment of the natural circulation within the TES in the first experimental tests has allowed to measure indirectly a heat exchange coefficient for a steady oil flow (hot/cold source flowing through the bottom/top heat exchanger). The temperature profile in the tank is detected near the lifts by 9 thermocouples indicated as A1-A9 in Fig. 1. The temperatures are detected for time intervals of the order of magnitude of the minute. The channels are isolated to lift the hot MS directly to the hot layer above as well as let the colder layers rapidly move downward to the bottom of the tank.

The model validation is obtained by correlating the results of two different discharging tests operating with the oil as the cold source (MS releasing thermal power to the fluid entering at 180 °C and exiting at 250 °C). The temperature profile is obtained by measuring the temperature at the thermocouple for 1-27 minutes (test 1) and 1- 16 min (test 2).

Fig. 2 depicts one of the two spiral heat exchangers (HE) of the TES. Fig. 2 (a) represents a detail of the submerged HE. The circulating MS enters from the side of the HE and crosses it in the radial direction in the HE shell (outside of the tubes). During the charging phase, the MS is heated by the hot oil flowing into the tubes and releasing the thermal power. Once heated, the warmer layer is pushed up to the hot layer by the buoyancy force. The hot source fluid flows inside the oil circuit of the 5 rings-spiral HE. Fig. 2 (b) shows the geometry and the related parameters of the equivalent "linearized" heat exchanger, object of the short-cut modelling here presented.
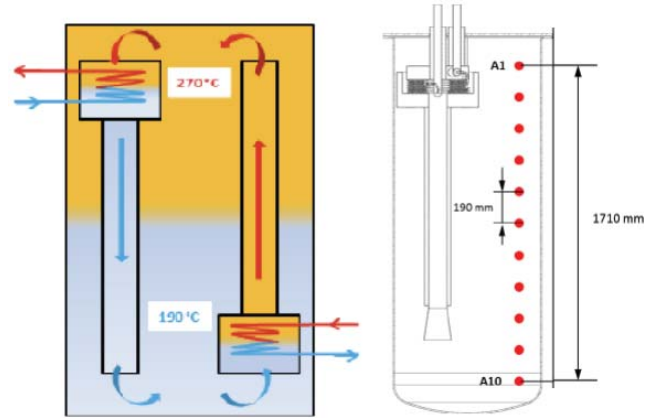

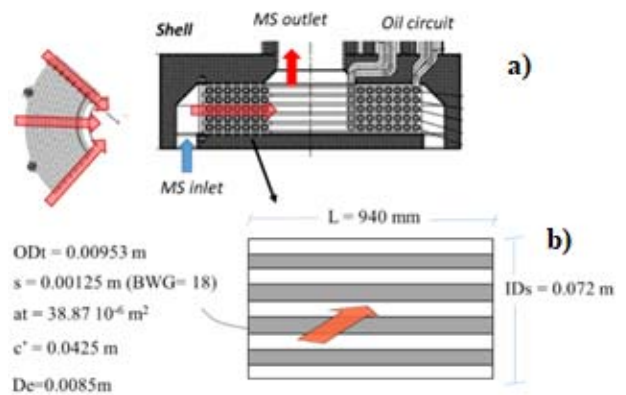Fig. 1 Schematic of the Thermocline Storage Tank Prototype realized by ENEA

$ODt = 0.00953$ m
$s = 0.00125$ m (BWG= 18)
$at = 38.87 \, 10^{-6}$ m²
$c' = 0.0425$ m
$De = 0.0085$ m

Fig. 2 Geometrical details of heat exchanger section and eqivalent scheme as Shell & Tube heat exchanger

III. MODELLING

The heat transfer model is based on the linearization of the exchanger in order to establish an analogy with the tube & shell heat exchanger as represented in Fig. 2 and the actual spiral exchanger installed in the tank with more complex fluid and thermal dynamics in order to obtain practical correlation between geometry and heat exchange and to optimize the apparatus.. The natural convection establishes the circulation of the bulk liquid MS and its flow across the transverse section of the tube bundle (in radial direction).

In this section, the following semi-empirical correlations based on the classical approach of Kern [20] are applied to the linearized shell & tube HE sketched in Fig. 2.

$$U_D = Q/(LMTD \cdot Ft \cdot A) \tag{1}$$

$$U_C = \left(\frac{1}{h_{io}} + \frac{1}{h_o}\right)^{-1} \tag{2}$$

$$Nu_t = \frac{h_i ID_t}{k_o} = 0.023 \cdot Re_o^{0.8} Pr_o^{0.33} \left(\frac{\mu}{\mu_w}\right)^{0.14} \tag{3}$$

$$Nu_s = \frac{h_o D_e}{k_{MS}} = 1.86 \cdot Re_{MS}^{0.33} Pr_{MS}^{0.33} \left(\frac{r}{L}\right)^{0.1} \tag{4}$$

World Academy of Science, Engineering and Technology
International Journal of Energy and Environmental Engineering
Vol:11, No:10, 2017

where Q is the HE duty, h_o is the shell-side coefficients, h_i is the tube-side coefficient estimated respectively through the for the forced convection correlation of the Nusselt number, Nu (3), (4). The dimensionless numbers occurring in the equations are calculated in stationary conditions for each experimental interval of time depending on the physical properties of the fluids (mean values as reported in Table I). The volumetric flow rate of the oil and the thermal power are known. The MS flow rate and of the salt mixture was assumed, depending on the natural circulation, to satisfy the energy balance. In other words, by applying the enthalpy balances on both the salt and the oil sides, it is possible to check the mass flow in play and to estimate the dimensionless numbers to calculate the heat transfer coefficients h_i and h_o according to (3), (4).

TABLE I
PHYSICAL PROPERTIES OF FLUIDS AT AVERAGE TEMPERATURE

Symbol	Oil	MS
$c_p [kJ/kg\ K]$	2.35	1.56
$\rho\ [kg/m3]$	810	1940
$\mu\ [Pa\ s]$	$0.25 \cdot 10^{-3}$	$7.50 \cdot 10^{-3}$
$k\ [W\ /mK]$	0.09	0.435

The validation is obtained by computing the "clean" exchange coefficient U_C and comparing it with the measurable "dirty" U_D value, estimated by the indirect measuring the thermal power through the flow rate and temperature of the fluid flowing into the tubes. These values diverge during the plant operation because of the fouling; in the case of our start-up tests these are similar. The correction factor F_t which, based on the actual heat exchange profile, reduces the logarithmic average delta (LMTD) is estimated based on the Trombone-cooler cross-flow model and is 0.97 for both tests [20]. For the calculation of the LMTD, the temperature values considered were the top temperature (detected at the thermocouple A2) and the HE-exit temperature (equal to the one detected at the bottom according to the hypothesis of adiabaticity in the tubes). The transverse cross-section between the tubes (spiral HE in Fig. 2) has been take into account.

$$v_{MS} = w_{MS}/(\rho_{MS} \cdot A_t) \tag{5}$$

$$A_t = L \cdot (ID_s - 5 \cdot OD_t) \tag{6}$$

From the point of view of the analytical characterization, the use of Normal or Logistic CDF functions have been recently used to dimensionless describe the thermocline [12], [13], [19]. Bayon et al. have tested these functions on Andasol plant by determining the dependence of the S variance parameter to the time (thermocline degradation function) [13] according to the following equation:

$$\theta = \left(1 + e^{-\frac{z*-zc*}{S}}\right)^{-1} \tag{7}$$

$$z* = z/L \tag{8}$$

$$t* = t\ D/L^2 \tag{9}$$

$$z_c * = v^* t^* \tag{10}$$

$$v* = (\rho\ c_p\ L\ v)/k \tag{11}$$

$$\theta = (T - Tmin)/(Tmax - Tmin) \tag{12}$$

where $\theta*$, $z*$ and z_c* are respectively the dimensional functions of the temperature T, the spatial depth/height z and the position of the thermocline, z_c. Therefore, the function (7) describing the temperature profile along the height z depends on the physical properties of the MS, the bulk velocity v_b of the salt inside the tank, and by the amplification parameter S, the only actual fitting parameter adjustable on experimental data. Both v_b and the parameter S can be related with a time variable for different plant solutions and operation conditions to produce short-cut evaluation of the storage performance [19]. As an example, through the estimation of S (influencing the rate of thermocline degradation), it is possible to evaluate the thermocline thickness (TC) as the portion of z which corresponds to 90% of the Global temperature gradient and to obtain its variation over the time [19].

$$TC = 2\ n\ S \ln(2 + \sqrt{3}) \tag{13}$$

IV. RESULTS AND DISCUSSION

The model validation is obtained by correlating the results of two different discharging tests operating with the oil as the cold source (acquiring the thermal power from 180 °C to 250 °C). The temperature profile during the time is reported in function of the thermocouple in Fig. 3, as well as in function of the vertical axis (at different times) in Fig. 4 for the test 1. These data showed the formation and migration of the thermocline from the bottom to the top, between two isothermal conditions representing the initial time where the MS is homogeneous at 290 °C and the end of the experiment where the MS temperature profile is almost constantly near the 280 °C. These data allowed to validate the heat transfer model, for the system tank – submerged HE, by comparing the calculated heat transfer coefficient U_C and the measured U_D. In the case of radial flow, the cross section is reduced during the salt passage through the HE with a consequent increase of the velocity, Re and Nu that assume takes higher values at the outlet with respect to the inlet of the HE. The calculations shown here have been repeated with different flow velocity; the best results coincide with the assumption of a "mean" cross flow velocity corresponding to a circumference of L = 0.650m (equivalent length of the linearized heat exchanger length of Fig. 2).

Fig. 4 reports the values of U_D (experimental) and U_C (calculated) for the two discharging tests. This comparison proofs the good correspondence between the model and the experimental data with similar values of the global coefficient U, around 400 W/m²K whereas the calculate inside coefficient h_i is 1690 W/m²K and the outside coefficient h_o is 635 W/m²K. Noteworthy is that the data were obtained in very similar conditions but with two different power levels: 17 kW

World Academy of Science, Engineering and Technology
International Journal of Energy and Environmental Engineering
Vol:11, No:10, 2017
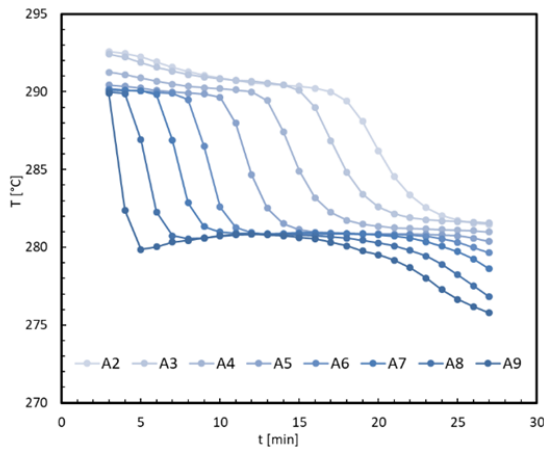
for test 1 and 27 kW for test 2.

Fig. 3 Temperature profile over the time detected at different
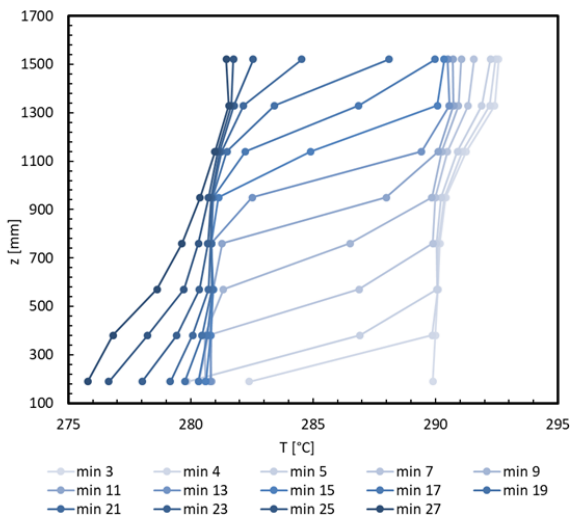thermocouples (test 1)

Fig. 4 Temperature profile versus the tank height at different time of
detection (test 2)

Although the exchange model should be validated by multiple tests as well as the charging phase, the results seem to demonstrate that the forced convection in the equivalent HE is a valid representation of the more complex nature of the phenomenon. The mathematical model (1)-(6) referring to the HE simplification of Fig. 3 can be therefore used for the scale-up of the exchangers and/or variation of geometry. At this point, the thermal profiles have been correlated with the above-mentioned logistic function in order to obtain a function characterizing the dynamics of thermal storage. An example of comparison between the calculated CDF function and the experimental data can be found for some time intervals of test 2 in Fig. 5. The parameter of the thermocline equation (7) are S=0.02 and the v_b (11) of the order of magnitude of 10^{-1} m/s. The geometry produces a stratification dynamic that can be well described with the proposed approach. The good overlap of the model on data has been obtained in the intermediate zones (both in time and space) because of the clear limits of

the model in predicting transitional data (time error) and border effects (error in space) mainly visible for the two upper thermocouples. The bulk velocity is similar for both tests and not far from the experimental estimation; the values over the time are reported in Fig. 7. Further experiments could produce a correlation between v_b and thermal power. More interestingly, it will be possible to study the bulk velocity for very distant thermal powers and in the case of simultaneous charging and discharging phases.
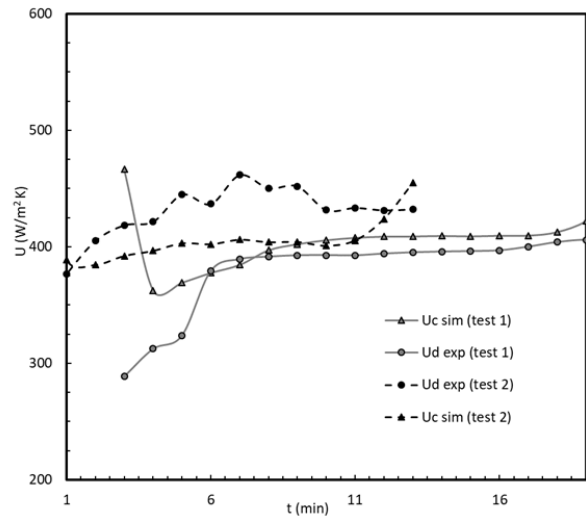

Fig. 5 Time variation of the calculated and measured global heat
transfer coefficient

The analytical description allows to estimate energy decay functions in the event of time as indicated by Pizzolato et al. [18]. The model for both cases has showed a "pseudo-linear" growth of TC over the time. As reported in the literature [5], it is possible to determine the performance of the Thermocline Exergetic Performance (TEP) through the study of the temporal trend of TC.
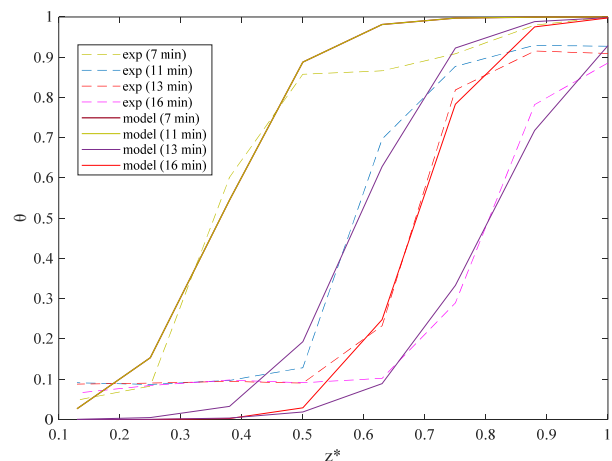

Fig. 6 Comparison of experimental data and reduced order model for
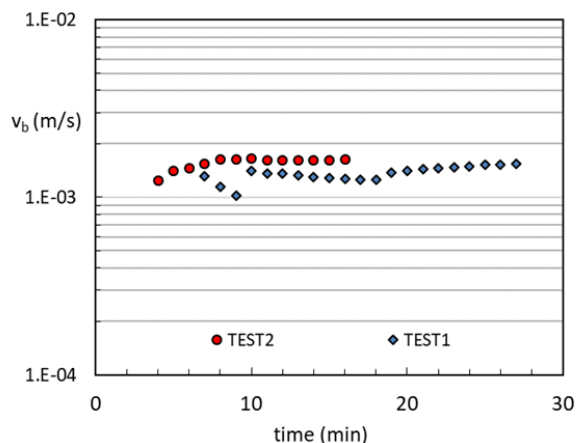TEST1 discharge test

World Academy of Science, Engineering and Technology
International Journal of Energy and Environmental Engineering
Vol:11, No:10, 2017

Fig. 7 Comparison between the estimated v_b for Test 1 and Test 2

REFERENCES

[1]   V Gadhamshetty, VG Gude, N. Nirmalakhandanc. Thermal energy storage system for energy conservation and water desalination in power plants, Energy 66 (2014), 938-949.

[2]   N. Ghaffour, S. Latteman, T.M. Missimer, K.C. Ng, S. Sinha, G. Amy. Renewable energy-driven innovative energy-efficient desalination technologies .Applied Energy136 (2014), 1155-1165.

[3]   CSP Alliance Report The Economic and Reliability Benefits of CSP with Thermal Energy Storage: LiteratureReview and Research Needs

[4]   IEA-ETSAP and IRENA© Technology Brief E10 – January 2013 www.etsap.org – www.irena.org, last access: 01-09-2017.

[5]   http://www.renewindians.com/2013/03/argest-csp-project-in-world-inaugrated-in-Abu-Dhabi.html, last access: 01-09-2017.

[6]   Renewables Global Status Report, REN21, 2017.

[7]   Pizzolato A., Donato F., Verda V., Santarelli M., Sciacovelli A. CSP plants with thermocline thermal energy storage and integrated steam generator – Techno-economic modeling and design optimization.Energy 139 2017.

[8]   De Falco, M., Capocelli, M., Giannattasio, A. Performance analysis of an innovative PCM-based device for cold storage in the civil air conditioning (2016) Energy and Buildings, 122, pp. 1-10.

[9]   M De Falco, M Capocelli, G Losito, V Piemonte. LCA perspective to assess the environmental impact of a novel PCM-based cold storage unit for the civil airconditioningJournal of Cleaner Production 165, 697-704.

[10] Capocelli M., Di Paola L., De Falco M., Piemonte V., Barba D. A novel process of humidification-dehumidification with brine recirculation for desalination in remote areas of the world. HDH Desalination and water treatment 69 (2017) 244-251.

[11] Di Patricia Palenzuela, Diego-César Alarcón-Padilla, Guillermo Zaragoza, Concentrating Solar Power and Desalination Plants: Engineering and Economics.

[12] R. Bayon, E. Rojas, Analytical description of thermocline tank performance in dynamic processes and stand-by periods, Energy Procedia, n. 57 (2014) 617- 626.

[13] R. Bayon, E. Rojas, Analytical function describing the behaviour of a thermocline storage tank: A requirement for annual simulations of solar thermal power plants, International Journal of Heat and Mass Transfer, n. 68 (2014) 641-648.

[14] G. Angelini, A. Lucchini, G. Manzolini. Comparison of thermocline molten salt storage performances to commercial two-tank configuration. Energy Procedia 49 (2014) 694 – 704.

[15] I. Hernández Arriaga, F. Zaversky, D. Astrain. Object-oriented modeling of molten-salt-based thermocline thermal energy storage for the transient performance simulation of solar thermal power plants. Energy Procedia 69 (2015) 879 – 890.

[16] Shin MS, Kim HS, Jang DS, Lee SN, Yoon HG. 2004. Numerical and experimental study on the design of a stratified thermal storage system. Applied Thermal Engineering. 24: 17-27.

[17] E. Rivas, E. Rojas, R. Bayón, W. Gaggioli, L. Rinaldi, F. Fabrizi. CFD model of a molten salt tank with integrated steam generator. Energy Procedia 49 (2014) 956 – 964.

[18] R. Bayon, E. Rivas, E. Rojas, Study of thermocline tank performance in dynamic processes and stand-by periods with an analytical function, Energy Procedia, n. 49 (2014) 725-734.

[19] A. Pizzolato, F. Donato, V. Verda, M. Santarelli, CFD-based reduced model for the simulation of thermocline thermal energy storage systems, Applied Thermal Engineering, n. 76 (2015) 391-399.

[20] D.Q. Kern. Process Heat Transfer (1950) McGraw-Hill Book co, Singapore.